Received: 24 April 2023 | Revised: 17 July 2023 | Accepted: 14 August 2023

DOI: 10.1111/cas.15944

ORIGINAL ARTICLE

Cancer Science WILEY

B7H3 increases ferroptosis resistance by inhibiting cholesterol metabolism in colorectal cancer

Haiyan Jin[1,2] | Mengxin Zhu[3] | Dongze Zhang[1,2] | Xiaoshan Liu[4] | Yuesheng Guo[4] | Lu Xia[3] | Yanjun Chen[3] | Yuqi Chen[1,3] | Ruyan Xu[1,2] | Cuiping Liu[1,2] | Qinhua Xi[1,3] | Suhua Xia[2,5] | Tongguo Shi[1,2] | Guangbo Zhang[1,2]

[1]Jiangsu Institute of Clinical Immunology, The First Affiliated Hospital of Soochow University, Suzhou, China

[2]Jiangsu Key Laboratory of Clinical Immunology, Soochow University, Suzhou, China

[3]Department of Gastroenterology, The First Affiliated Hospital of Soochow University, Suzhou, China

[4]Pasteurien College, Suzhou Medical College, Soochow University, Suzhou, China

[5]Department of Oncology, The First Affiliated Hospital of Soochow University, Suzhou, China

Correspondence

Guangbo Zhang and Tongguo Shi, Jiangsu Institute of Clinical Immunology, The First Affiliated Hospital of Soochow University, 178 East Ganjiang Road, Suzhou 215000, China.

Email: 15962265210@163.com: shitg@suda.edu.cn

Suhua Xia, Department of Oncology, The First Affiliated Hospital of Soochow University, 188 Shizi Road, Suzhou 215000, China.

Email: xiasuhua@suda.edu.cn

Funding information

Gusu Talent Project of Suzhou, Grant/Award Number: SGSWS2020011; Jiangsu Provincial Medical Key Discipline, Grant/Award Number: ZDXK202246; Natural Science Foundation Project of the Doctoral Cultivation Program, Grant/Award Number: BXQN202119; Suzhou "Science and Education Revitalize Health" Youth Science and Technology Project, Grant/Award Number: KJXW2022005; Suzhou Natural Science Foundation, Grant/Award Number: sky2022046 and sky2022128; the key project of Jiangsu Provincial Health and wellness

Abstract

Ferroptosis, a newly discovered form of regulated cell death, has been reported to be associated with multiple cancers, including colorectal cancer (CRC). However, the underlying molecular mechanism is still unclear. In this study, we identified B7H3 as a potential regulator of ferroptosis resistance in CRC. B7H3 knockdown decreased but B7H3 overexpression increased the ferroptosis resistance of CRC cells, as evidenced by the expression of ferroptosis-associated genes (*PTGS2*, *FTL*, *FTH*, and *GPX4*) and the levels of important indicators of ferroptosis (malondialdehyde, iron load). Moreover, B7H3 promoted ferroptosis resistance by regulating sterol regulatory element binding protein 2 (SREBP2)-mediated cholesterol metabolism. Both exogenous cholesterol supplementation and treatment with the SREBP2 inhibitor betulin reversed the effect of B7H3 on ferroptosis in CRC cells. Furthermore, we verified that B7H3 downregulated SREBP2 expression by activating the AKT pathway. Additionally, multiplex immunohistochemistry was carried out to show the expression of B7H3, prostaglandin-endoperoxide synthase 2, and SREBP2 in CRC tumor tissues, which was associated with the prognosis of patients with CRC. In summary, our findings reveal a role for B7H3 in regulating ferroptosis by controlling cholesterol metabolism in CRC.

Abbreviations: CRC, colorectal cancer; DEG, differentially expressed gene; FTH, ferritin heavy chain; FTL, ferritin light chain; GO, Gene Ontology; GPX4, glutathione peroxidase 4; GSH, glutathione; HMGCR, 3-hydroxy-3-methylglutaryl-CoA reductase; HMGCS, 3-hydroxy-3-methylglutaryl-CoA synthase; HO-1, heme oxygenase-1; IHC, immunohistochemistry; LDL-C, low-density lipoprotein cholesterol; LDLR, low-density lipoprotein receptor; MDA, malondialdehyde; mIHC, multiplex immunohistochemistry; NC, negative control; Nrf2, nuclear factor erythroid 2-related factor 2; n-SREBP2, nuclear SREBP2; PTGS2, prostaglandin-endoperoxide synthase 2; qPCR, quantitative PCR; RCD, regulated cell death; RNA-seq, RNA sequencing; ROS, reactive oxygen species; SQLE, squalene epoxidase; SREBP2, sterol regulatory element binding protein 2; T-CHO, total cholesterol.

Haiyan Jing and Mengxin Zhu contributed equally.

Commission, Grant/Award Number: zd2021050; The National Natural Science Foundation of China, Grant/Award Number: 81872328

KEYWORDS
B7H3, cholesterol, CRC, ferroptosis, SREBP2

1 | INTRODUCTION

Colorectal cancer is one of the leading causes of cancer-related death worldwide,[1] with nearly 2 million newly diagnosed cases each year.[2] Although the diagnosis and treatment methods have improved significantly, conventional treatments, including endoscopic and surgical local excision, chemotherapy, radiotherapy, Chinese medicine treatment, and immunotherapy, have limited effects on patients with advanced CRC. Hence, it is an urgent need to identify new targets and understand their molecular mechanisms in CRC progression.

Ferroptosis is considered a novel form of RCD that is distinct from necroptosis, apoptosis, and autophagy.[3] Ferroptosis is caused by the accumulation of intracellular iron, which promotes lipid peroxidation and leads to cell death.[4] Iron metabolism, GSH/GPX4 pathway activity, and lipid metabolism are the main factors involved in ferroptosis.[5] Recent studies have reported that a novel ferroptosis-related gene signature can be a good biomarker for predicting the prognosis of patients with CRC.[6,7] Wei et al. indicated that tagitinin C, a sesquiterpene lactone, induced ferroptosis through endoplasmic reticulum stress-mediated activation of the protein kinase RNA-like endoplasmic reticulum kinase (PERK)-Nrf2-HO-1 signaling pathway in CRC cells.[8] These studies suggest that ferroptosis plays a key role in modulating CRC progression. However, the molecular mechanism of the regulation of ferroptosis in CRC remains unclear.

B7H3, also named CD276, was described as a member of the B7 cosignaling molecule family.[9] B7H3 has classic extracellular immunoglobulin variable (IgV)-like and immunoglobulin constant (IgC)-like domains.[10] Numerous cancer studies have reported a strong link between dysregulated B7H3 expression and cancer-related biological functions such as cell survival, proliferation, metastasis, and drug resistance.[11] For example, B7H3 expression in ovarian cancer cells contributed to CC motif chemokine ligand 2-CC motif chemokine receptor 2-M2 macrophage axis-mediated immunosuppression and tumor progression.[12] Moreover, a recent study reported that B7H3 overexpression was positively correlated with CD31 levels, and confirmed that the B7H3/nuclear factor-κB/vascular endothelial growth factor A axis promoted CRC angiogenesis.[13]

Interestingly, B7H3 was found to be associated with GSH and lipid metabolism in adipocytes and lung cancer cells,[14,15] implying that B7H3 might modulate ferroptosis. In this study, we investigated whether and how B7H3 affects ferroptosis resistance in CRC. B7H3 silencing promoted but B7H3 overexpression inhibited RSL3-induced ferroptosis in CRC cells by regulating AKT/SREBP2 axis-mediated cholesterol metabolism. Moreover, we evaluated the prognostic impact of B7H3, SREBP2, and PTGS2 expression by mIHC in CRC patients. The results showed the $B7H3^{-}PTGS2^{+}SREBP2^{+}$ low group had a significantly worse prognosis. This knowledge reveals that B7H3/AKT/SREBP2 signaling exerts crucial effects on cholesterol metabolism and ferroptosis, possibly providing promising targets for CRC treatment.

2 | MATERIALS AND METHODS

2.1 | Cell lines and cell culture

The human normal colon epithelial cell (NCM460) and five CRC cell lines (RKO, HCT116, HT29, SW480, and SW620) were purchased from ATCC and cultured in DMEM (#L310KJ; Shanghai Basalmedia Technologies Co., Ltd) and RPMI-1640 (#L220KJ; Shanghai Basalmedia Technologies Co., Ltd) medium containing 10% FBS (#04-001-1ACS; Biological Industries) and 1% penicillin and streptomycin (#C0222; Beyotime) at 37°C in a humidified atmosphere of 5% CO_2.

2.2 | Xenograft tumor model

All experiments involving live mice were approved by the Institutional Animal Care and Use Committee at Soochow University. Six- to eight-week-old female BALB/c nude mice were purchased from Suzhou Sinosure Biotechnology Co., Ltd. All mice were maintained in a specific pathogen-free environment. To investigate the effect of B7H3 on ferroptosis and cholesterol metabolism, the mice were fed a high-cholesterol diet (#D12079B; Research Diets) for 3 weeks before establishment of the xenograft tumor model. A total of 5×10^6 B7H3 knockdown (shB7H3) or NC HCT116 cells were injected s.c. into the axilla of the mouse. Tumor volume (mean ± SEM; mm^3) was calculated according to the following equation: $V\,(mm^3)=S^2\,(mm^2)\times L$ (mm)/2, where S and L are the smallest and the largest perpendicular tumor diameters, respectively.[16] After 18 days, the mice were killed and the tumor specimens were weighed. Additionally, the xenograft tumor tissues were used for MDA, iron, and IHC assays.

2.3 | RNA sequencing assay

For RNA-seq analysis, equal amounts of shB7H3 HCT116 cells and control cells were used for RNA extraction. The RNA-seq analysis was carried out by GENEWIZ Biotech Co.

2.4 | Immunohistochemistry

Briefly, the xenograft tumor samples were sliced into 5 μm-thick sections. The sections were incubated with a rabbit anti-mouse PTGS2

Ab (1:200, #12375-1-AP; Proteintech) and a rabbit anti-mouse SREBP2 Ab (1:200, #28212-1-AP; Proteintech) overnight at 4°C. This step was followed by staining (1 h at 37°C) with an HRP-conjugated rabbit anti-goat secondary Ab (Gene Company Limited). Next, the sections were visualized by staining with 3,3′-diaminobenzidine (Biocare Medical) and counterstaining with hematoxylin (#C0105S-1; Beyotime). The scoring criteria for PTGS2 and SREBP2 immunostaining were based on clinical data and adopting the semiquantitative immunoreactive score system.[17] Briefly, category A (intensity of immunostaining) was scored using the following criteria: 0, negative; 1, weak; 2, moderate; and 3, strong. Category B (percentage of immunoreactive cells) was scored using the following criteria: 1, 0%–25%; 2, 26%–50%; 3, 51%–75%; and 4, 76%–100%. Final scores were calculated by multiplying the scores of categories A and B in the same section; the scores ranged from 0 to 12.

2.5 | Multiplex immunohistochemistry

Human tissue microarrays containing 89 samples of CRC and 84 samples of matched adjacent normal tissue were obtained from Shanghai Outdo Biotech Co., Ltd. The expression of B7H3, PTGS2, and SREBP2 in the tissue microarray was analyzed by mIHC at Shanghai Outdo Biotech. Correlations of expression with clinicopathological parameters are shown in Table S2. Ethics approval was obtained from the Institutional Review Board of The First Affiliated Hospital of Soochow University. Informed consent was also obtained from the patients for the use of their data for experimentation.

2.6 | Other methods

Detail descriptions of other methods used in this study are provided in supplemental materials and methods and Table S1.

2.7 | Statistical analysis

Data were obtained from three independent experimental replicates. All statistical data were analyzed with GraphPad Prism 7.0. Student's *t*-test was used for comparisons between two groups, and one-way ANOVA was used for comparisons among more than two groups. The results are expressed as the mean ± SD. $p < 0.05$ was considered statistically significant.

3 | RESULTS

3.1 | B7H3 knockdown promotes ferroptosis in CRC cells

To select suitable cell lines for the in vitro experiments, the level of B7H3 protein was detected in human normal colon epithelial cells NCM460 and several CRC cell lines including RKO, HCT116, HT29, SW480, and SW620. Compared with NCM460 cells, B7H3 expression was higher in RKO, HCT116, HT29, and SW480 cells. Moreover, among these CRC cell lines, B7H3 expression levels were higher in RKO and HCT116 cells than in other cell lines (Figure 1A). To explore the effects of B7H3 on ferroptosis in CRC cells, stable B7H3 knockdown HCT116 and RKO cell lines were established using a lentiviral delivery system. Western blot, flow cytometry, and RT-qPCR analyses confirmed that both the protein (Figure 1B,C) and mRNA (Figure 1D) levels of B7H3 were significantly decreased in CRC cells. Morphological observation indicated that RSL3 addition caused cells to shrink (Figure 1E). The image count results indicate a significant decrease in the number of surviving cells after B7H3 knockdown (Figure S1A). As shown in Figure 1F,G, knockdown of B7H3 significantly enhanced RSL3-induced growth inhibition in CRC cells. In addition, knockdown of B7H3 increased the MDA content and iron in CRC cells treated with RSL3 (Figure 1H,I). Next, we analyzed the expression of ferroptosis-related genes, including *PTGS2*, *FTL*, *FTH*, and *GPX4*, in B7H3-knockdown CRC cells by RT-qPCR. As shown in Figure 1J, reduced expression of B7H3 led to increases in the expression of *PTGS2*, *FTL*, and *FTH* and a decrease in the expression of *GPX4* in HCT116 cells. The expression of *PTGS2*, *FTL*, and *FTH* was also significantly increased in B7H3 knockdown RKO cells (Figure 1K). But B7H3 deletion had no influence on *GPX4* expression in RKO cells (Figure 1K). In summary, these data indicate that B7H3 knockdown increases CRC cell sensitivity to ferroptosis.

3.2 | B7H3 overexpression suppresses ferroptosis in CRC cells

Next, we constructed HCT116 and RKO cells with stable B7H3 overexpression by infecting them with the B7H3 overexpression lentivirus. As shown in Figure 2A–C, both the protein and mRNA levels of B7H3 were significantly increased in CRC cells with stable B7H3 overexpression. Overexpression of B7H3 significantly increased the the number of surviving cells (Figures 2D and S1B) and attenuated RSL3-induced growth inhibition in CRC cells (Figure 2E,F). Moreover, the results of the MDA (Figure 2G) and iron assays (Figure 2H) showed that B7H3 overexpression markedly reduced ferroptosis in CRC cells incubated with RSL3. In addition, B7H3 overexpression decreased the expression of PTGS2, FTL, and FTH and increased the expression of GPX4 in CRC cells (Figure 2I,J). Collectively, these results indicate that B7H3 overexpression increases ferroptosis resistance in CRC cells.

3.3 | B7H3 suppresses cholesterol biosynthesis in CRC cells

To investigate the mechanism by which B7H3 regulates ferroptosis in CRC cells, we undertook RNA-seq using sh-B7H3 and NC HCT116 cells. As shown in Figure 3A, a total of 1729 significant DEGs (fold change >1 and $p < 0.05$) were identified. Among them,

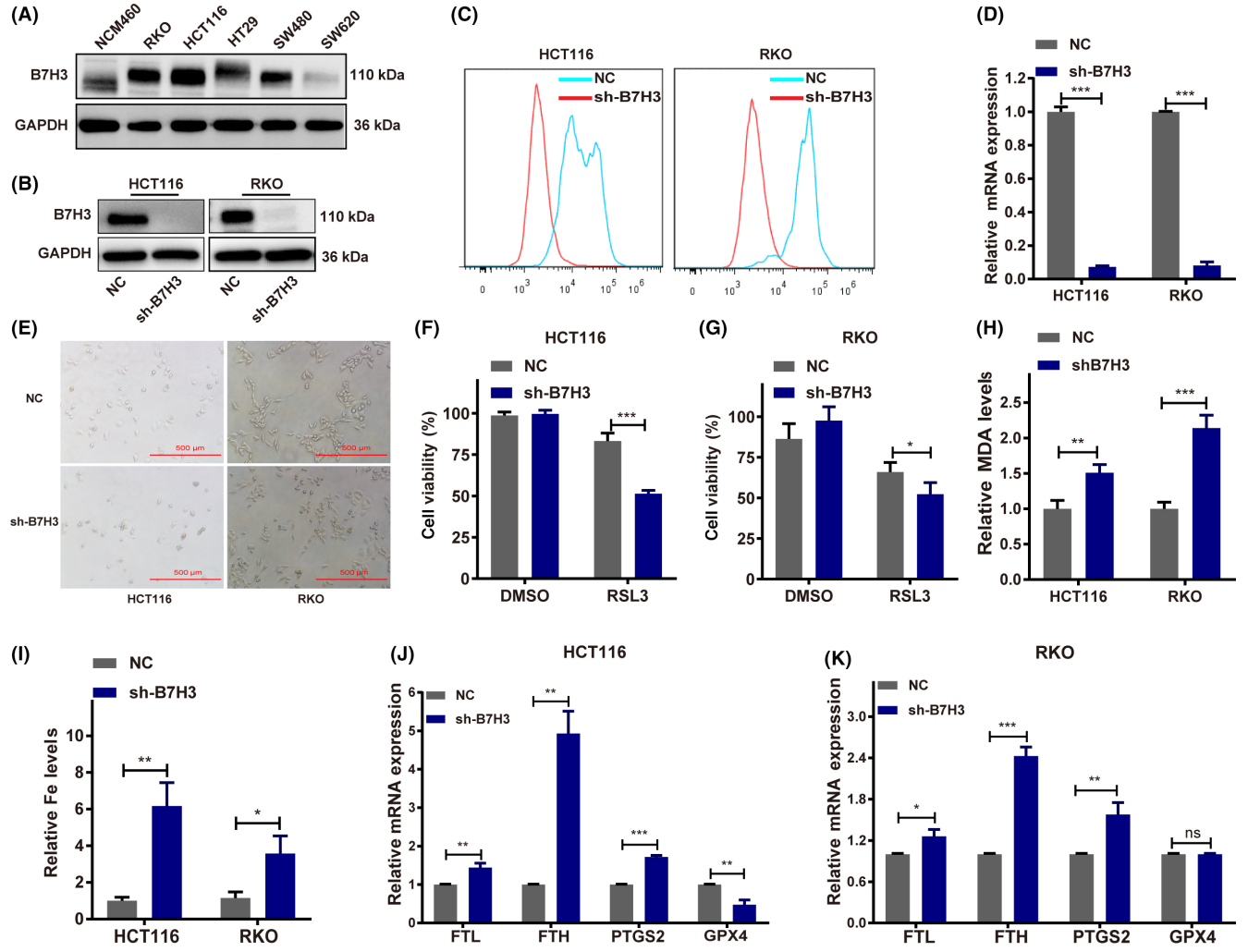

FIGURE 1 B7H3 knockdown promotes ferroptosis in colorectal cancer. (A) B7H3 protein levels in NCM460, RKO, HCT116, HT29, HCT8, SW480, and SW620 cells were analyzed by western blotting. (B, C) Protein expression of B7H3 in HCT116 and RKO cells treated with B7H3 shRNA (sh-B7H3) or negative control RNA (NC) was analyzed by (B) western blotting and (C) flow cytometry. (D) mRNA levels of B7H3 in HCT116 and RKO cells transfected with sh-B7H3 or NC were measured by RT-quantitative PCR (qPCR). (E) Representative images of HCT116 and RKO cells cotreated with sh-B7H3 and RSL3 (5 μM). (F, G) Viability of (F) HCT116 and (G) RKO cells treated with RSL3 was tested by CCK-8 assay. (H) Malondialdehyde (MDA) content and (I) iron load in HCT116 and RKO cells cotreated with sh-B7H3 and RSL3 (5 μM). (J, K) mRNA expression of ferritin light chain (FTL), ferritin heavy chain (FTH), prostaglandin-endoperoxide synthase 2 (PTGS2), and glutathione peroxidase 4 (GPX4) in HCT116 (J) and RKO (K) cells cotreated with sh-B7H3 and RSL3 (5 μM) was measured by RT-qPCR. Results are presented as mean ± SD. $^{*}p < 0.05$, $^{**}p < 0.01$, $^{***}p < 0.001$. ns, not significant.

1029 were upregulated and 700 were markedly downregulated (Figure 3A). Furthermore, the results of GO functional enrichment analysis indicated that the DEGs were markedly involved in cholesterol-related processes, including cholesterol homeostasis, cholesterol import, cholesterol biosynthetic process, and regulation of cholesterol biosynthetic process (Figure 3B). The Sankey diagram (Figure 3C) shows the distribution of the hub genes in cholesterol metabolism: 7-dehydrocholesterol reductase (*DHCR7*), farnesyl diphosphate farnesyltransferase 1 (*FDFT1*), *HMGCR*, *HMGCS1*, *SQLE*, and *SREBP2*.

We further demonstrated the effect of B7H3 on cholesterol metabolism in CRC cells. As shown in Figures 3D–F and S2, B7H3 knockdown significantly increased the T-CHO and LDL-C level in HCT116 and RKO cells. In contrast, B7H3 overexpression had the opposite effect (Figure S3A–D). Additionally, B7H3 knockdown increased but B7H3 overexpression decreased the expression of cholesterol metabolism-related genes (e.g., *SQLE*, *SREBP2*, *HMGCS*, and *LDLR*) in HCT116 and RKO cells (Figures 3G,H and S3E,F). Taken together, these results indicate that B7H3 plays an inhibitory role in cholesterol metabolism in CRC.

3.4 | B7H3 regulates ferroptosis through cholesterol metabolism

As reported, SREBP2, as a transcription factor, mediates the expression of multiple cholesterol metabolism-related genes (e.g., *LDLR*, *HMGCR*, and *CYP51A*) and plays key roles in the regulation of

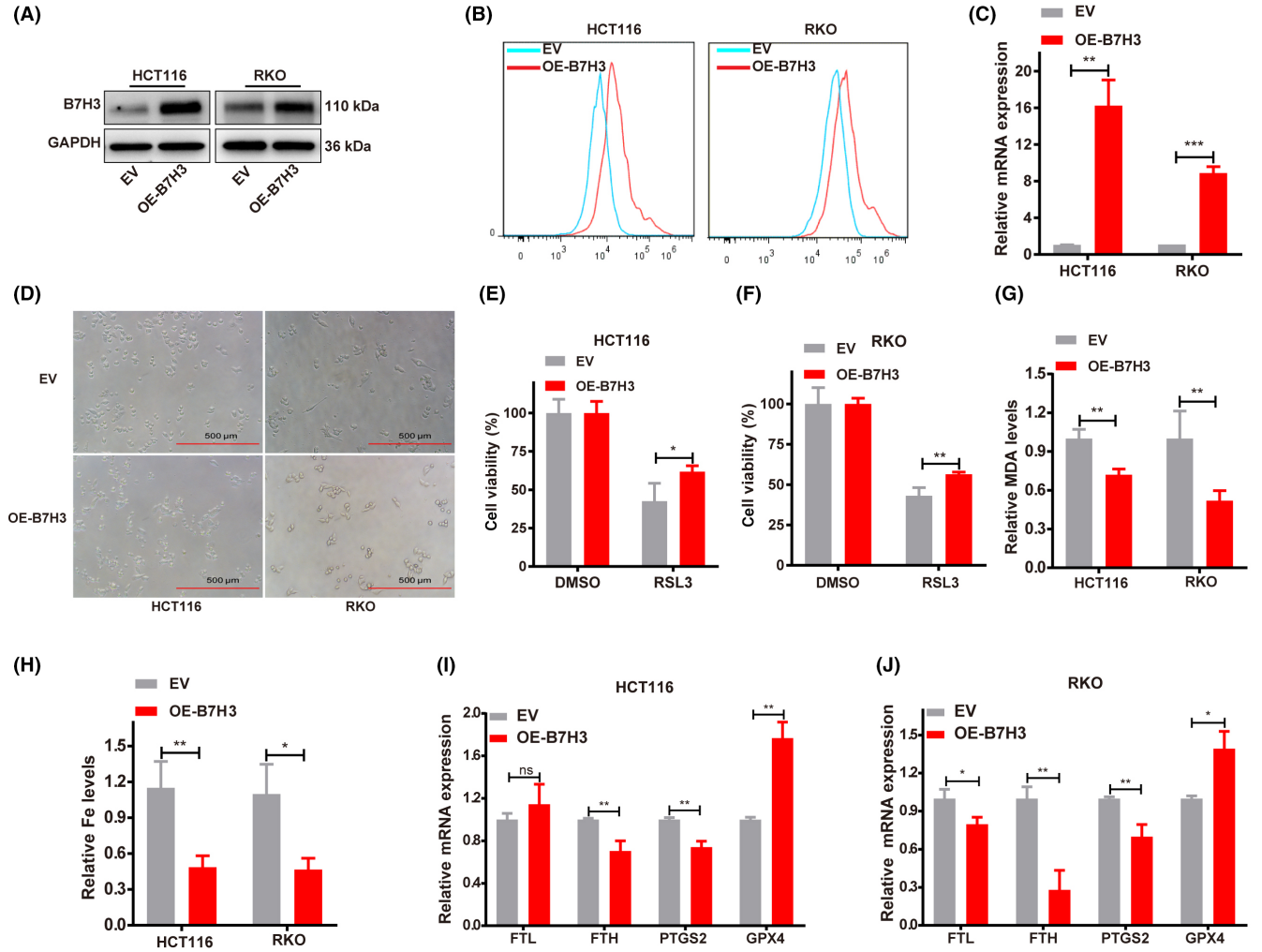

FIGURE 2 B7H3 overexpression suppresses ferroptosis in colorectal cancer cells. (A, B) Protein levels of B7H3 in HCT116 and RKO cells with stable B7H3 overexpression (OE-B7H3) were analyzed by (A) western blotting and (B) flow cytometry. (C) mRNA levels of B7H3 in HCT116 and RKO cells with OE-B7H3 were measured by RT-quantitative PCR (qPCR). (D) Representative images of HCT116 or RKO cells cotreated with OE-B7H3 and RSL3 (5 μM). (E, F) Viability of HCT116 (E) and RKO (F) cells treated with RSL3 was tested by CCK-8 assay. (G) Malondialdehyde (MDA) content and (H) iron load in HCT116 and RKO cells treated with RSL3 (5 μM). (I, J) mRNA expression of ferritin light chain (FTL), ferritin heavy chain (FTH), prostaglandin-endoperoxide synthase 2 (PTGS2), and glutathione peroxidase 4 (GPX4) in (I) HCT116 and (J) RKO cells treated with RSL3 (5 μM) was measured by RT-qPCR. Results are presented as mean ± SD. $^{*}p < 0.05$, $^{**}p < 0.01$, $^{***}p < 0.001$. EV, empty vector; ns, not significant.

cholesterol metabolism.[18] Given that B7H3 knockdown increased the SREBP2 mRNA level in CRC cells (Figure 3G,H), we wondered whether B7H3 modulates cholesterol metabolism and ferroptosis in CRC cells in an SREBP2-dependent manner. As shown in Figure 4A, n-SREBP2 protein expression was significantly upregulated in CRC cells after B7H3 knockdown. In contrast, the protein level of n-SREBP2 was markedly decreased in B7H3-overexpressing CRC cells (Figure 4B). Importantly, treatment with betulin, an inhibitor of SREBP2, significantly reduced the T-CHO and LDL-C levels, which were increased in HCT116 and RKO cells after B7H3 knockdown (Figure 4C,D). Betulin addition abolished the effect of B7H3 on the MDA and iron content in HCT116 and RKO cells (Figure 4E,F). In addition, the effect of B7H3 overexpression on reducing the T-CHO and LDL-C levels was reversed by exogenous cholesterol supplementation (Figure S4A,B). Moreover, exogenous cholesterol supplementation abolished the B7H3-induced decreases in the MDA and iron contents (Figure S4C,D). These results suggest that B7H3 inhibits ferroptosis by inhibiting cholesterol metabolism through SREBP2.

Then, we attempted to explore the signaling pathway by which B7H3 controls SREBP2 expression. Previous studies have shown that SREBP2 can be modulated by AKT in cancer cells.[19,20] Indeed, knockdown of B7H3 expression decreased the activity of p-AKT (Figure 4A). Conversely, B7H3 overexpression was accompanied by increased p-AKT activity (Figure 4B). Moreover, we observed that perifosine, an AKT phosphorylation inhibitor, significantly increased the expression of n-SREBP2 in B7H3-overexpressing CRC cells. These results indicate that B7H3 could regulate the expression of SREBP2 through the AKT signaling pathway in CRC cells.

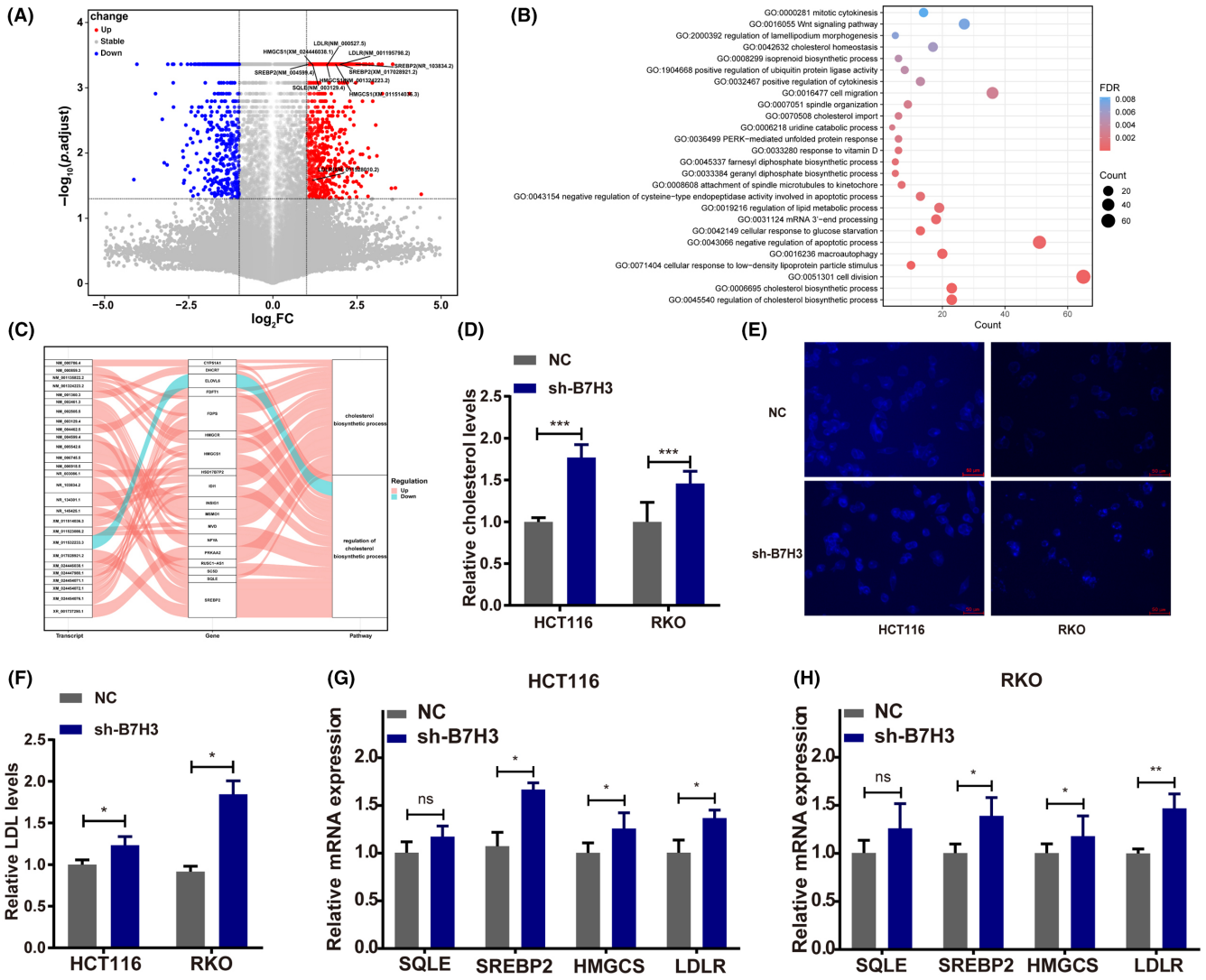

FIGURE 3 B7H3 suppresses cholesterol metabolism. (A) Differentially expressed genes (DEGs) between negative control (NC) and shB7H3 HCT116 cells are shown in a volcano plot. Red dots represent upregulated DEGs; blue dots represent downregulated DEGs. (B) Bubble plots of the Gene Ontology biological process enrichment analysis. (C) Sankey diagram showing the connections among cholesterol metabolism-related hub genes. (D) Total cholesterol levels in B7H3 knockdown HCT116 and RKO cells. (E) Free cholesterol concentrations in B7H3 knockdown HCT116 and RKO cells were determined by filipin III staining. (F) Low-density lipoprotein (LDL) cholesterol levels in B7H3 WT and knockdown HCT116 and RKO cells were examined. (G, H) Expression of cholesterol metabolism-related genes (*SQLE*, *SREBP2*, *HMGCS*, *LDLR*) in B7H3-knockdown (G) HCT116 and (H) RKO cells was measured by RT-quantitative PCR. Results are presented as mean ± SD. $^{*}p < 0.05$, $^{**}p < 0.01$, $^{***}p < 0.001$. FC, fold change; FDR, false discovery rate; ns, not significant.

3.5 | B7H3 is associated with cholesterol metabolism and ferroptosis in CRC cells in vivo

To investigate the effect of B7H3 on ferroptosis and cholesterol metabolism in vivo, nude mice were fed a high-cholesterol diet 2 weeks before the xenograft models of B7H3-knockdown HCT116 tumors and control tumors were established. The tumor images, sizes, and weights showed that B7H3 knockdown markedly inhibited HCT116 tumor growth (Figure 5A–C). Downregulation of B7H3 did not change tumor size or weight under normal diet (Figure S5). Then, the expression of SREBP2 and PTGS2 in xenograft tumor tissues was examined by IHC. The results showed that both SREBP2 and PTGS2 expression was significantly increased in the B7H3-knockdown HCT116 group compared with the control group (Figure 5D–F). Although there was no significant difference in the iron load between the control group and the B7H3-knockdown HCT116 group (Figure 5G), the MDA content in the B7H3-knockdown HCT116 group was markedly higher than that in the control group (Figure 5H). These results together suggest that B7H3 is involved in ferroptosis and cholesterol metabolism in vivo.

3.6 | $B7H3^{-}PTGS2^{+}SREBP2^{+}$ cells promote an improved prognosis in CRC patients

Next, we determined B7H3, PTGS2, and SREBP2 expression in 89 samples of primary CRC tumor tissues and 84 samples of adjacent

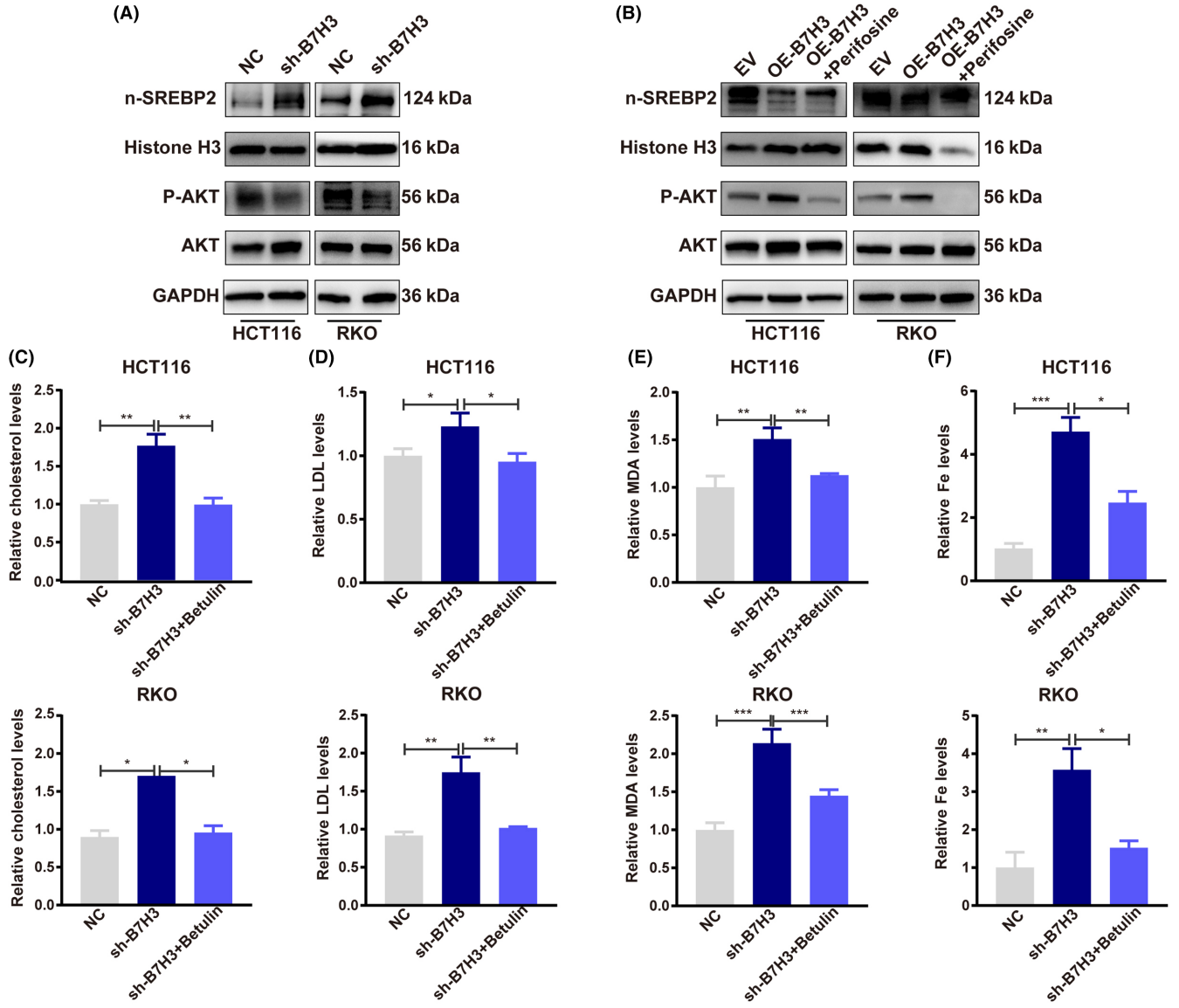

FIGURE 4 B7H3 regulates ferroptosis through cholesterol metabolism. (A) Protein levels of nuclear sterol regulatory element binding protein 2 (n-SREBP2), p-AKT, and AKT in B7H3 knockdown HCT116 and RKO cells. Histone H3 served as a nuclear loading control. GAPDH served as a loading control. (B) Protein levels of n-SREBP2, p-AKT, and AKT in B7H3-overexpressing HCT116 and RKO cells. Histone H3 served as a nuclear loading control. GAPDH served as a loading control. (C) Total cholesterol and (D) low-density lipoprotein (LDL) cholesterol levels in B7H3 knockdown HCT116 and RKO cells after treatment with 4 μm betulin for 48 h. (E) Malondialdehyde (MDA) and (F) total iron content in B7H3 knockdown HCT116 and RKO cells cotreated with RSL3 and betulin. Results are presented as mean ± SD. $^{*}p < 0.05$, $^{**}p < 0.01$, $^{***}p < 0.001$. NC, negative control.

normal tissues by mIHC. Representative images of B7H3, PTGS2, and SREBP2 staining in the matched tumor tissues and adjacent tissues are shown in Figure 6A,B. Significantly, B7H3 was aberrantly expressed in CRC tissues compared with normal tissues, and the patients with high B7H3^{+} cells predicted a shorter fraction survival compared with the patients with low B7H3^{+} cells (Figure 6C,D). There was no difference in the proportion of PTGS2^{+} cells between cancer and paracancerous tissue and had no influence on the survival of patients (Figure S6A,B). The SREBP2^{+} cells increased in tumor tissues but did not affect survival of patients (Figure S6C,D). As shown in Figure S6E,F, there was no correlation between B7H3^{+} with PTGS2^{+} or SREBP2^{+} in CRC tissues. Given that B7H3 negatively regulated PTGS2 and SREBP2 expression in HCT116 and RKO cells, the proportion of B7H3^{-}PTGS2^{+}SREBP2^{+} cells in tumor tissues and adjacent normal tissues was analyzed. As shown in Figure 6E, the proportion of B7H3^{-}PTGS2^{+}SREBP2^{+} cells was significantly lower in tumor tissues than in adjacent normal tissues. Moreover, the patients were classified into two groups by the B7H3^{-}PTGS2^{+}SREBP2^{+} expression pattern, namely, the B7H3^{-}PTGS2^{+}SREBP2^{+} low group (proportion ≤ median value) and the B7H3^{-}PTGS2^{+}SREBP2^{+} high group (proportion > median value) group. The results of Kaplan–Meier survival analysis showed that patients in the B7H3^{-}PTGS2^{+}SREBP2^{+} low group had a significantly worse prognosis than those in the B7H3^{-}PTGS2^{+}SREBP2^{+} high group (Figure 6F).

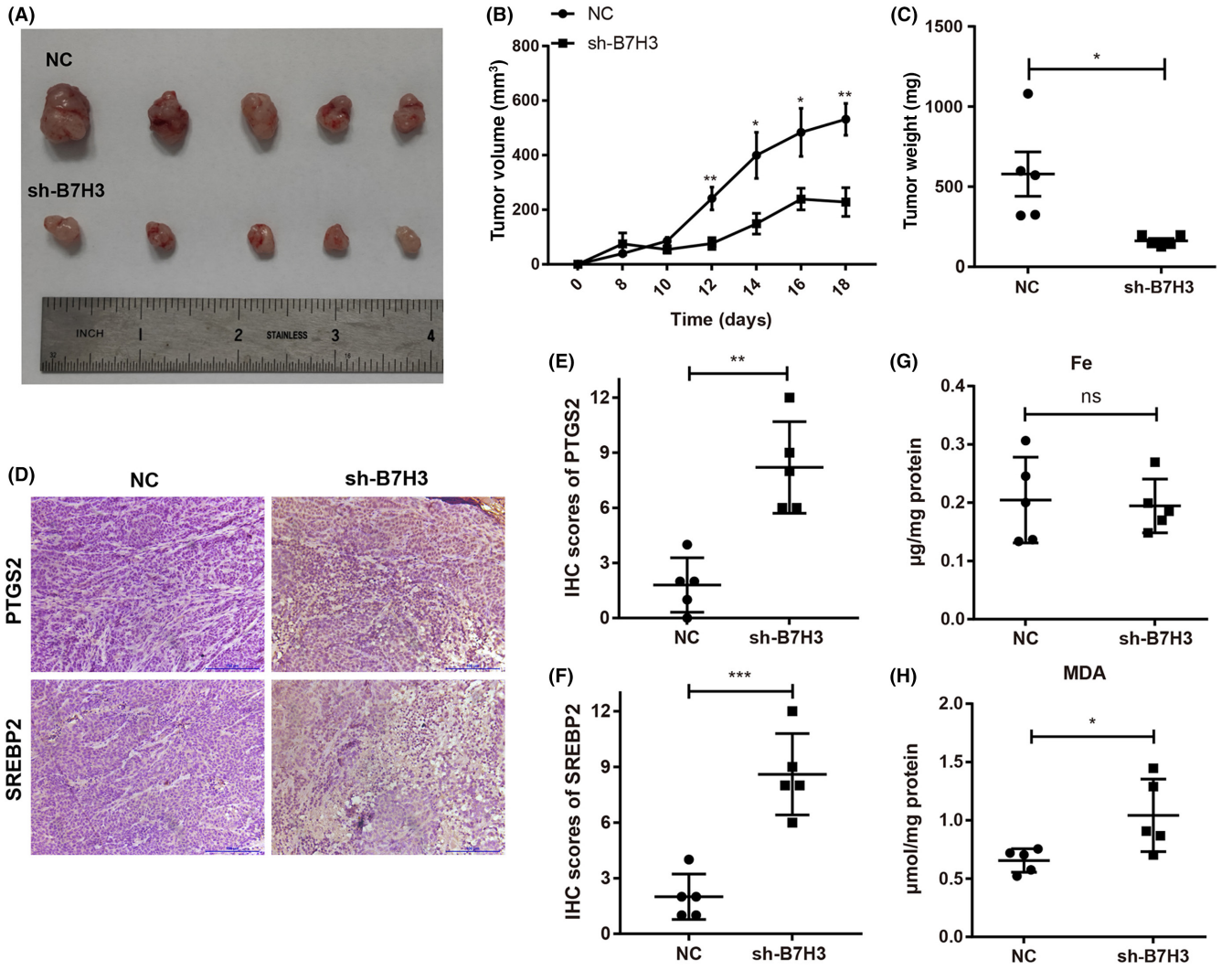

FIGURE 5 B7H3 is involved in ferroptosis and cholesterol metabolism in colorectal cancer cells in vivo. (A) Representative images of B7H3-knockdown HCT116 tumors in nude mice fed a high cholesterol diet. (B) Volumes of B7H3-knockdown HCT116 tumors in nude mice fed a high cholesterol diet. (C) Weights of B7H3-knockdown HCT116 tumors in nude mice fed a high cholesterol diet. (D) Images of immunohistochemical (IHC) analysis of sterol regulatory element binding protein 2 (SREBP2) and prostaglandin-endoperoxide synthase 2 (PTGS2) protein expression in tumor tissue of nude mice fed a high cholesterol diet ($n = 5$). One representative image of each is shown. (E) PTGS2 and (F) SREBP2 protein expression based on the IHC staining index in tumor tissues of the xenograft model. (G) Total iron and (H) malondialdehyde (MDA) content was measured in tumor tissues of nude mice fed a high cholesterol diet ($n = 5$). Results are presented as mean ± SEM. $^{*}p < 0.05$, $^{**}p < 0.01$. NC, negative control; ns, not significant.

4 | DISCUSSION

An increasing number of investigations have discovered that ferroptosis is associated with the occurrence and progression of CRC and could be a potential new target for CRC therapy.[21] For instance, increased expression of TIGAR in CRC tissues was found to induce resistance to ferroptosis in CRC cells through the ROS/AMP kinase/SCD1 signaling pathway.[22] Wang et al. noted that serine and arginine-rich splicing factor 9 (SFRS9) overexpression suppressed ferroptosis induced by erastin and sorafenib in CRC cells by elevating GPX4 protein expression.[23] In addition, cetuximab enhanced ferroptosis induced by RSL3 in *KRAS* mutant CRC cells by blocking the Nrf2/HO-1 axis through p38 MAPK activation.[24] In the current study, we found that B7H3 silencing promoted but B7H3 overexpression inhibited RSL3-induced ferroptosis in CRC cells, as evidenced by the expression of ferroptosis-associated genes (*PTGS2*, *FTL*, *FTH*, and *GPX4*) and the levels of important indicators of ferroptosis (MDA and iron load). Interestingly, we observed that knockdown of B7H3 had no influence on the GPX4 mRNA expression in RKO cells, a key regulator of ferroptosis.[25] Given that the regulation of ferroptosis is complex and involved in multiple molecular mechanisms,[26,27] we speculated that B7H3 modulated ferroptosis in CRC cells in a GPX4-independent manner. Further investigation is needed in our future study. Previous studies indicated that B7H3 is involved in multiple forms of RCDs, such as apoptosis and autophagy.[28,29] Therefore, we concluded that B7H3 is a key regulator of RCD, including ferroptosis.

Cholesterol is an essential component of the mammalian cell membrane,[30] and aberrant cholesterol metabolism has been

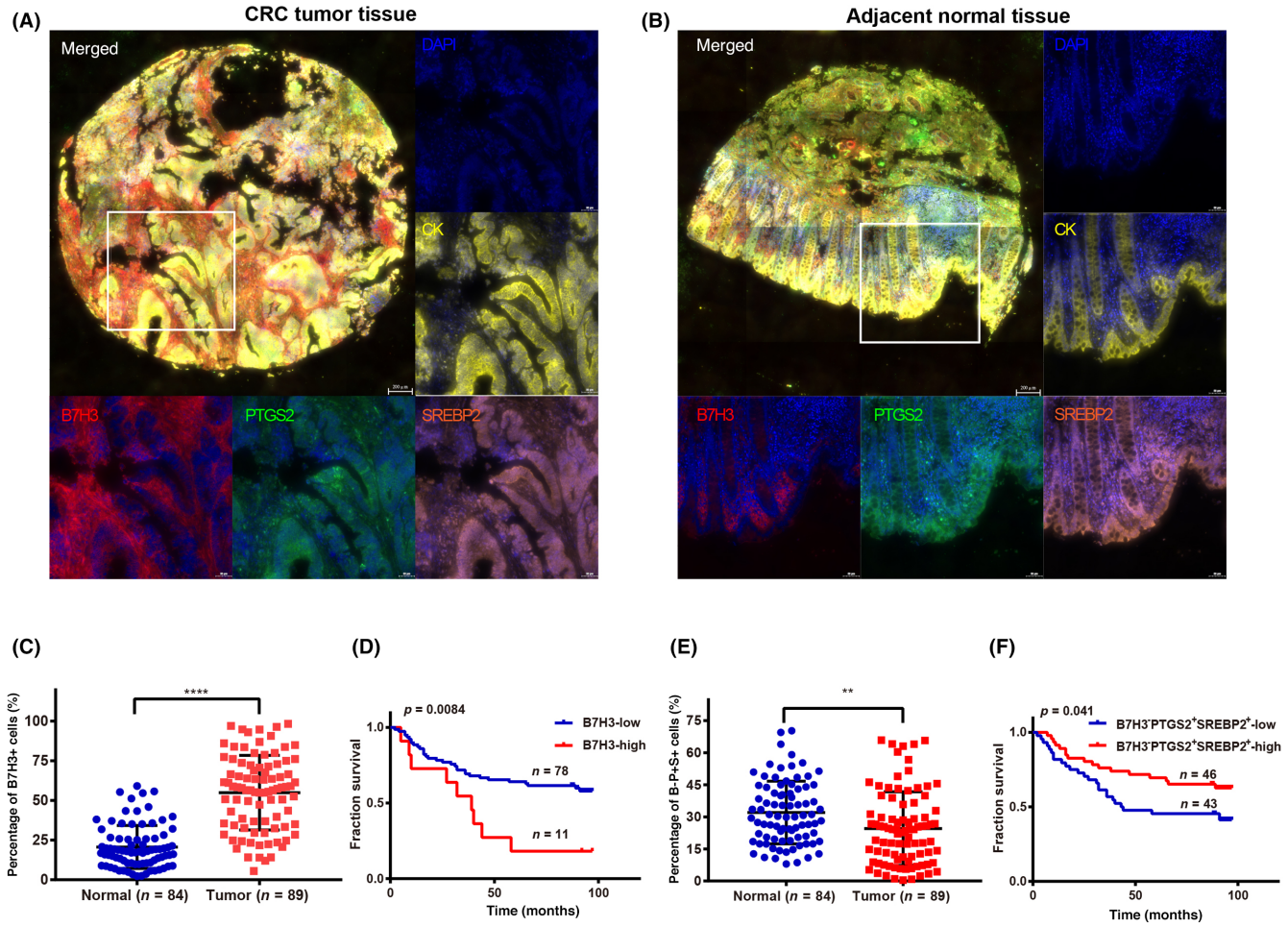

FIGURE 6 B7H3$^-$ prostaglandin-endoperoxide synthase 2 (PTGS2)$^+$ sterol regulatory element binding protein 2 (SREBP2)$^+$ cells promote an improved prognosis in colorectal cancer (CRC) patients. (A, B) Representative images of multiplex immunohistochemistry assay of B7H3 (red), PTGS2 (green), and SREBP2 (orange) expression in (A) CRC tumor tissue and (B) adjacent normal tissue. Nuclei and tumor epithelial cells are marked by DAPI (blue) and cytokeratin (CK; yellow), respectively. Scale bar, 50 μm. (C) Percentages of B7H3$^+$ cells in tumor tissues ($n = 89$) and normal tissues ($n = 84$). (D) Kaplan–Meier analysis of the survival rate of 89 CRC patients stratified according to the B7H3$^+$ cells level. (E) Percentages of B7H3$^-$ PTGS2$^+$SREBP2$^+$ cells in tumor tissues ($n = 89$) and normal tissues ($n = 84$). (F) Kaplan–Meier analysis of the survival rate of 89 CRC patients stratified into B7H3$^-$ PTGS2$^+$SREBP2$^+$ cells low (proportion ≤ median value) and B7H3$^-$ PTGS2$^+$SREBP2$^+$ cells high (proportion > median value)groups. Results are presented as mean ± SD. $^{**}p < 0.01$, $^{****}p < 0.0001$.

shown to be linked to the occurrence and development of various cancers, such as hepatocellular carcinoma, glioblastoma, ovarian cancer, and CRC.[31–34] For example, hepatocyte growth factor activated SREBP2-dependent cholesterol biosynthesis, which was required for the colonization and growth of metastatic CRC cells in the liver.[35] It has been reported that genetic and pharmacological inhibition of cholesterol biosynthesis reduced the self-renewal capacity and tumorigenic potential of colon spheroid models in vitro and in vivo.[36] Herein, RNA-seq analysis was used to investigate the mechanism by which B7H3 regulates ferroptosis in CRC cells. The GO enrichment analysis showed that DEGs in B7H3 knockdown HCT116 cells were associated with cholesterol metabolism. A recent study showed that chronic exposure of cancer cells to 27-hydroxycholesterol (27-HC), an abundant circulating cholesterol metabolite, resulted in increased tumor metastatic capacity and ferroptosis resistance.[31] Therefore, we inferred that B7H3 inhibits ferroptosis in CRC cells by modulating cholesterol metabolism. Our results showed that blockade of cholesterol metabolism using betulin, an inhibitor of SREBP2, significantly abated B7H3 knockdown-mediated ferroptosis in CRC cells, while exogenous cholesterol supplementation obviously reversed the effects of B7H3 overexpression on ferroptosis. Importantly, B7H3 knockdown markedly inhibited HCT116 tumor growth under a high-cholesterol diet. Moreover, B7H3 deletion significantly upregulated PTGS2 expression and MDA levels in xenograft tumor tissues. However, there was no significant difference in the iron load between the control group and the B7H3-knockdown xenograft tumor. Given that B7H3 knockdown increased, while B7H3 overexpression decreased, iron content in HCT116 and RKO cells in vitro, we inferred that B7H3 might regulate the iron levels in other cell types, such as immune cells, endothelial cells, and fibroblasts, in the xenograft tumor tissues. It would be interesting to further

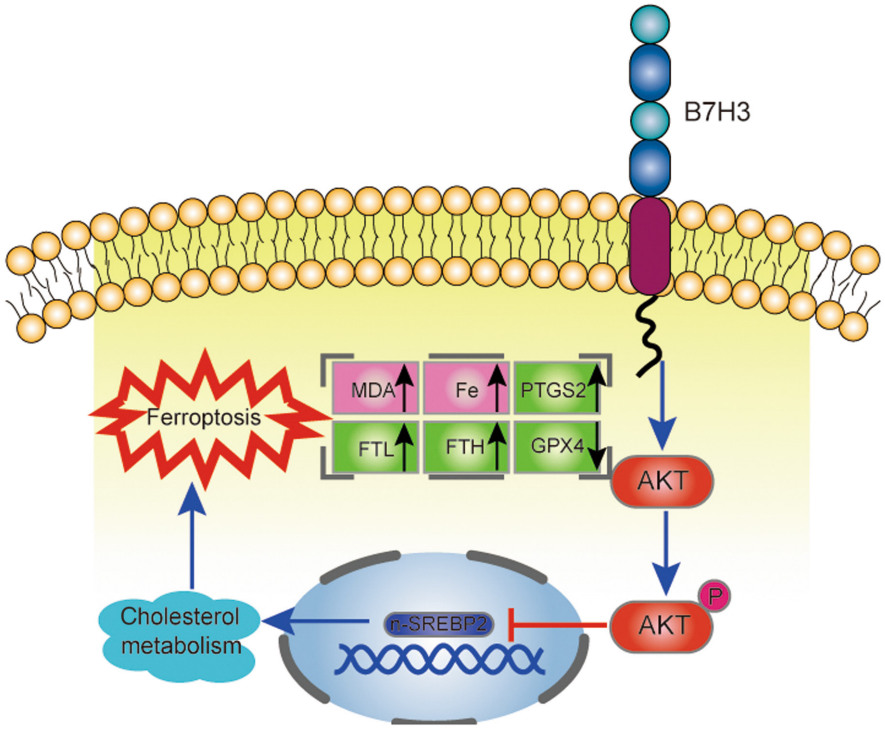

FIGURE 7 Schematic diagram of the proposed mechanism by which B7H3 inhibits ferroptosis through cholesterol metabolism in colorectal cancer cells through the AKT/sterol regulatory element binding protein 2 (SREBP2) pathway. FTH, ferritin heavy chain; FTL, ferritin light chain; GPX4, glutathione peroxidase 4; MDA, malondialdehyde; PTGS2, prostaglandin-endoperoxide synthase 2.

elaborate the roles of B7H3 in modulating ferroptosis in immune cells, endothelial cells, or fibroblasts in CRC. Considering that both B7H3 and cholesterol metabolism participated in the regulation of apoptosis and autophagy,[29,37–39] we could not rule out that B7H3 knockdown suppressed xenograft tumor growth through modulating apoptosis or autophagy under a high-cholesterol diet. Further investigation is needed in our future study. Hence, our findings indicate that B7H3 suppresses ferroptosis in CRC cells through cholesterol metabolism, and B7H3 silencing led to a decrease in xenograft tumor growth partly by regulating ferroptosis under a high-cholesterol diet.

A basic helix–loop–helix leucine zipper transcription factor, SREBP2, mainly regulates genes involved in cholesterol biosynthesis and homeostasis.[40] In prostate cancer, knockdown or inhibition of SREBP2 enhanced fluvastatin-induced cancer cell death.[41] A recent study reported that SREBP2 was crucial for enhancing cholesterol biosynthesis and lipid accumulation as well as tumorigenesis in hepatocellular carcinoma cells.[42] Notably, SREBP2 induces the transcription of the iron carrier transferrin, thereby conferring resistance to ferroptosis on circulating tumor cells in melanoma.[43] In the present study, the protein expression of nuclear SREBP2 was negatively related to B7H3 expression in CRC cells. Moreover, the SREBP2 inhibitor betulin markedly abolished the effects of B7H3 knockdown on cholesterol metabolism and ferroptosis in CRC cells. Therefore, our data suggest that B7H3 contributes to the ferroptosis resistance of CRC cells through SREBP2-mediated cholesterol metabolism. Additionally, silencing B7H3 affected the expression of other cholesterol metabolism-related genes (e.g., *SQLE*, *HMGCS*, and *LDLR*). We cannot exclude the possibility that B7H3 could modulate cholesterol metabolism and ferroptosis in CRC cells through *SQLE*, *HMGCS*, or *LDLR*. Further investigation is needed in our future study.

Accumulating studies have shown that SREBP2 expression is regulated by the AKT signaling pathway in cancer. In ovarian cancer, mitochondrial elongation factor 2 (MIEF2) upregulated SREBP expression to promote cell growth and metastasis by activating the ROS/AKT/mTOR signaling pathway.[19] In addition, PTEN/p53 deficiency ultimately promoted tumor cell growth and survival by activating SREBP transcription through the PI3K/AKT/glycogen synthase kinase 3β-mediated proteasome pathway.[20] Moreover, oncogenic activation of PI3K-AKT-mTOR signaling protected cancer cells against oxidative stress and ferroptosis through SREBP1-mediated lipogenesis.[44] Our previous studies showed that B7H3 overexpression promoted the activation of the AKT pathway in CRC cells.[45] Therefore, we concluded that B7H3 inhibits SREBP2 expression through the AKT pathway in CRC. Our results indicated that B7H3 negatively regulates SREBP2 expression in CRC cells by activating the AKT pathway, but further studies are needed to elucidate the molecular mechanisms underlying these associations.

In summary, our study reveals the regulatory role and mechanism of B7H3 in inhibiting ferroptosis in CRC cells. Depletion of B7H3 in CRC cells promotes ferroptosis through AKT/SREBP2 pathway-mediated cholesterol metabolism (Figure 7). Therefore, strategies to target B7H3/AKT/SREBP2 pathway-regulated ferroptosis could facilitate the development of effective therapeutics for CRC.

AUTHOR CONTRIBUTIONS

Suhua Xia, Tongguo Shi, and Guangbo Zhang performed study concept and design. Haiyan Jin and Mengxin Zhu performed most of the experiments and analyzed the data. Dongze Zhang, Xiaoshan Liu, Yuesheng

Guo, Lu Xia, Yanjun Chen, Yuqi Chen, Ruyan Xu, Cuiping Liu, and Qinhua Xi performed a specific subset of the experiments and analyses.

ACKNOWLEDGMENTS

Not applicable.

FUNDING INFORMATION

This work was supported by: the key project of Jiangsu Provincial Health and Wellness Commission (zd2021050); Jiangsu Provincial Medical Key Discipline (ZDXK202246); Suzhou Natural Science Foundation (sky2022046, sky2022128); the National Natural Science Foundation of China (81872328); Suzhou "Science and Education Revitalize Health" Youth Science and Technology Project (KJXW2022005); Gusu Talent Project of Suzhou (SGSWS2020011); and the Natural Science Foundation Project of the Doctoral Cultivation Program (BXQN202119).

CONFLICT OF INTEREST STATEMENT

The authors have declared that no competing interest exists.

ETHICS STATEMENT

Approval of the research protocol by an institutional reviewer board: Ethics approval was obtained from the Institutional Review Board of The First Affiliated Hospital of Soochow University.

Informed consent: Informed consent was obtained from the patients for use of their data for experimentation.

Registry and registration no. of the study/trial: N/A.

Animal studies: All experiments involving live mice were approved by the Institutional Animal Care and Use Committee at Soochow University.

ORCID

Xiaoshan Liu https://orcid.org/0009-0009-9774-3911
Tongguo Shi https://orcid.org/0000-0002-5382-2775

REFERENCES

1. Younis N, Roumieh R, Bassil E, Ghoubaira J, Kobeissy F, Eid A. Nanoparticles: attractive tools to treat colorectal cancer. *Semin Cancer Biol*. 2022;86:1-13.
2. Snyder M, Iraola-Guzmán S, Saus E, Gabaldón T. Discovery and validation of clinically relevant long non-coding RNAs in colorectal cancer. *Cancer*. 2022;14(16):3866. doi:10.3390/cancers14163866
3. Dixon SJ, Lemberg KM, Lamprecht MR, et al. Ferroptosis: an iron-dependent form of nonapoptotic cell death. *Cell*. 2012;149(5):1060-1072.
4. Wang X, Wang Z, Cao J, Dong Y, Chen Y. Ferroptosis mechanisms involved in hippocampal-related diseases. *Int J Mol Sci*. 2021;22(18):9902. doi:10.3390/ijms22189902
5. Hu W, Liang K, Zhu H, Zhao C, Hu H, Yin S. Ferroptosis and its role in chronic diseases. *Cell*. 2022;11(13):2040. doi:10.3390/cells11132040
6. Shao Y, Jia H, Huang L, et al. An original ferroptosis-related gene signature effectively predicts the prognosis and clinical status for colorectal cancer patients. *Front Oncol*. 2021;11:711776.
7. Qi X, Wang R, Lin Y, et al. A ferroptosis-related gene signature identified as a novel prognostic biomarker for colon cancer. *Front Genet*. 2021;12:692426.
8. Wei R, Zhao Y, Wang J, et al. Tagitinin C induces ferroptosis through PERK-Nrf2-HO-1 signaling pathway in colorectal cancer cells. *Int J Biol Sci*. 2021;17(11):2703-2717.
9. Chapoval A, Ni J, Lau J, et al. B7-H3: a costimulatory molecule for T cell activation and IFN-gamma production. *Nat Immunol*. 2001;2(3):269-274.
10. Vigdorovich V, Ramagopal UA, Lazar-Molnar E, et al. Structure and T cell inhibition properties of B7 family member, B7-H3. *Structure*. 2013;21(5):707-717.
11. Kanchan R, Doss D, Khan P, Nasser M, Mahapatra S. To kill a cancer: targeting the immune inhibitory checkpoint molecule, B7-H3. *Biochim Biophys Acta Rev Cancer*. 2022;1877(5):188783.
12. Miyamoto T, Murakami R, Hamanishi J, et al. B7-H3 suppresses antitumor immunity via the CCL2-CCR2-M2 macrophage axis and contributes to ovarian cancer progression. *Cancer Immunol Res*. 2022;10(1):56-69.
13. Wang R, Ma Y, Zhan S, et al. B7-H3 promotes colorectal cancer angiogenesis through activating the NF-κB pathway to induce VEGFA expression. *Cell Death Dis*. 2020;11(1):55.
14. Picarda E, Galbo P, Zong H, et al. The immune checkpoint B7-H3 (CD276) regulates adipocyte progenitor metabolism and obesity development. *Sci Adv*. 2022;8(17):eabm7012.
15. Luo D, Xiao H, Dong J, et al. B7-H3 regulates lipid metabolism of lung cancer through SREBP1-mediated expression of FASN. *Biochem Biophys Res Commun*. 2017;482(4):1246-1251.
16. Shi T, Ma Y, Cao L, et al. B7-H3 promotes aerobic glycolysis and chemoresistance in colorectal cancer cells by regulating HK2. *Cell Death Dis*. 2019;10(4):308.
17. Liu M, Huang F, Zhang D, et al. Heterochromatin protein HP1γ promotes colorectal cancer progression and is regulated by miR-30a. *Cancer Res*. 2015;75(21):4593-4604.
18. Goedeke L, Canfrán-Duque A, Rotllan N, et al. MMAB promotes negative feedback control of cholesterol homeostasis. *Nat Commun*. 2021;12(1):6448.
19. Zhao S, Cheng L, Shi Y, Li J, Yun Q, Yang H. MIEF2 reprograms lipid metabolism to drive progression of ovarian cancer through ROS/AKT/mTOR signaling pathway. *Cell Death Dis*. 2021;12(1):18.
20. Shangguan X, Ma Z, Yu M, Ding J, Xue W, Qi J. Squalene epoxidase metabolic dependency is a targetable vulnerability in castration-resistant prostate cancer. *Cancer Res*. 2022;82(17):3032-3044.
21. Liang X, You Z, Chen X, Li J. Targeting ferroptosis in colorectal cancer. *Metabolites*. 2022;12:8.
22. Liu MY, Li HM, Wang XY, et al. TIGAR drives colorectal cancer ferroptosis resistance through ROS/AMPK/SCD1 pathway. *Free Radic Biol Med*. 2022;182:219-231.
23. Wang R, Xing R, Su Q, et al. Knockdown of SFRS9 inhibits progression of colorectal cancer through triggering ferroptosis mediated by GPX4 reduction. *Front Oncol*. 2021;11:683589.
24. Yang J, Mo J, Dai J, et al. Cetuximab promotes RSL3-induced ferroptosis by suppressing the Nrf2/HO-1 signalling pathway in KRAS mutant colorectal cancer. *Cell Death Dis*. 2021;12(11):1079.
25. Seibt T, Proneth B, Conrad M. Role of GPX4 in ferroptosis and its pharmacological implication. *Free Radic Biol Med*. 2019;133:144-152.
26. Tang D, Chen X, Kang R, Kroemer G. Ferroptosis: molecular mechanisms and health implications. *Cell Res*. 2021;31(2):107-125.
27. Chen X, Kang R, Kroemer G, Tang D. Broadening horizons: the role of ferroptosis in cancer. *Nat Rev Clin Oncol*. 2021;18(5):280-296.
28. Zhou X, Ouyang S, Li J, et al. The novel non-immunological role and underlying mechanisms of B7-H3 in tumorigenesis. *J Cell Physiol*. 2019;234(12):21785-21795.
29. Zhang M, Zhang H, Fu M, et al. The inhibition of B7H3 by 2-HG accumulation is associated with downregulation of VEGFA in IDH mutated gliomas. *Front Cell Dev Biol*. 2021;9:670145.
30. Simons K, Ikonen E. How cells handle cholesterol. *Science*. 2000;290(5497):1721-1726.

31. Liu W, Chakraborty B, Safi R, Kazmin D, Chang CY, McDonnell DP. Dysregulated cholesterol homeostasis results in resistance to ferroptosis increasing tumorigenicity and metastasis in cancer. *Nat Commun*. 2021;12(1):5103.
32. Fang R, Chen X, Zhang S, et al. EGFR/SRC/ERK-stabilized YTHDF2 promotes cholesterol dysregulation and invasive growth of glioblastoma. *Nat Commun*. 2021;12(1):177.
33. Criscuolo D, Avolio R, Calice G, et al. Cholesterol homeostasis modulates platinum sensitivity in human ovarian cancer. *Cell*. 2020;9(4):828. doi:10.3390/cells9040828
34. Jun SY, Brown AJ, Chua NK, et al. Reduction of squalene epoxidase by cholesterol accumulation accelerates colorectal cancer progression and metastasis. *Gastroenterology*. 2021;160(4):1194-1207 e28.
35. Zhang KL, Zhu WW, Wang SH, et al. Organ-specific cholesterol metabolic aberration fuels liver metastasis of colorectal cancer. *Theranostics*. 2021;11(13):6560-6572.
36. Gao S, Soares F, Wang S, et al. CRISPR screens identify cholesterol biosynthesis as a therapeutic target on stemness and drug resistance of colon cancer. *Oncogene*. 2021;40(48):6601-6613.
37. Li Q, Zhong X, Yao W, et al. Inhibitor of glutamine metabolism V9302 promotes ROS-induced autophagic degradation of B7H3 to enhance antitumor immunity. *J Biol Chem*. 2022;298(4):101753.
38. Wang Y, Liu C, Hu L. Cholesterol regulates cell proliferation and apoptosis of colorectal cancer by modulating miR-33a-PIM3 pathway. *Biochem Biophys Res Commun*. 2019;511(3):685-692.
39. Shao W, Zhu W, Luo M, et al. Cholesterol suppresses GOLM1-dependent selective autophagy of RTKs in hepatocellular carcinoma. *Cell Rep*. 2022;39(3):110712.
40. Xue L, Qi H, Zhang H, et al. Targeting SREBP-2-regulated mevalonate metabolism for cancer therapy. *Front Oncol*. 2020;10:1510.
41. Longo J, Mullen P, Yu R, et al. An actionable sterol-regulated feedback loop modulates statin sensitivity in prostate cancer. *Mol Metab*. 2019;25:119-130.
42. Wei M, Nurjanah U, Herkilini A, et al. Unspliced XBP1 contributes to cholesterol biosynthesis and tumorigenesis by stabilizing SREBP2 in hepatocellular carcinoma. *Cell Mol Life Sci*. 2022;79(9):472.
43. Hong X, Roh W, Sullivan R, et al. The lipogenic regulator SREBP2 induces transferrin in circulating melanoma cells and suppresses ferroptosis. *Cancer Discov*. 2021;11(3):678-695.
44. Yi J, Zhu J, Wu J, Thompson CB, Jiang X. Oncogenic activation of PI3K-AKT-mTOR signaling suppresses ferroptosis via SREBP-mediated lipogenesis. *Proc Natl Acad Sci U S A*. 2020;117(49):31189-31197.
45. Wang R, Sun L, Xia S, et al. B7-H3 suppresses doxorubicin-induced senescence-like growth arrest in colorectal cancer through the AKT/TM4SF1/SIRT1 pathway. *Cell Death Dis*. 2021;12(5):453.

SUPPORTING INFORMATION

Additional supporting information can be found online in the Supporting Information section at the end of this article.

How to cite this article: Jin H, Zhu M, Zhang D, et al. B7H3 increases ferroptosis resistance by inhibiting cholesterol metabolism in colorectal cancer. *Cancer Sci*. 2023;114:4225-4236. doi:10.1111/cas.15944